Octahedral μ-oxalato–nickel(II) dinuclear complexes with water and tridentate amines as blocking ligands: magnetostructural correlations

Albert Escuer*, Ramon Vicente and Joan Ribas
Departament de Química Inorgànica, Universitat de Barcelona, Diagonal 647, 08028-Barcelona (Spain)

Joel Jaud and Bernard Raynaud
Centre d'Elaboration de Matériaux et d'Etudes structurales du CNRS, PB 4347, 31055 Toulouse Cédex (France)

(Received July 8, 1993, revised September 14, 1993)

Abstract

Three nickel(II) dinuclear oxalato (ox) bridged compounds: (μ-ox)[Ni(dpt)(H_2O)]$_2$(ClO_4)$_2$ (**1**), (μ-ox)[Ni(Medpt)(H_2O)]$_2$(ClO_4)$_2$·2H_2O (**2**) and (μ-ox)[Ni(ept)(H_2O)]$_2$(ClO_4)$_2$ (**3**) have been synthesized and characterized where dpt is bis(3-aminopropyl)amine, Medpt is 3,3'-diamino-*N*-methyl-dipropylamine and ept is *N*-(2-aminoethyl)-1,3-propanediamine. The crystal structures of **1** and **2** have been solved Complex **1** crystallizes in the monoclinic system, space group *I2/a*, with FW=702.8, a=12 534(4), b=16.871(5), c=13.450(4) Å, β=95.28(7)°, V=2831(3) Å^3, Z=4, R=0.063 and R_w=0.068. Complex **2** crystallizes in the monoclinic system, space group $P2_1/n$, with FW=766.9, a=6.404(2), b=13.333(4), c=18.687(4) Å, β=97.67(8)°, V=1576(2) Å^3, Z=2, R=0 063 and R_w=0.068 In both complexes the nickel atom is placed in a distorted octahedral environment. The magnetic properties of these compounds have been investigated. The $\chi_M T$ versus T plots for **1–3** exhibit the typical shapes for antiferromagnetically coupled nickel(II) dinuclear complexes. The J values for **1–3** were −24.7, −21.6 and −25.0 cm^{-1}, respectively. These values are significantly lower than those reported for nickel(II) dinuclear complexes when the blocking ligands have four N atoms. The influence of the change in the electronegativity of the peripheral ligand atoms on the magnetic behaviour has been studied by means of extended-Huckel calculations

Key words. Crystal structures; Nickel complexes; Oxalato complexes; Dinuclear complexes

Introduction

The published magnetic studies on dinuclear nickel(II) oxalato bridged compounds [1–8] show that this ligand causes a relatively strong antiferromagnetic coupling between two nickel(II) centres. The fully studied compounds are all octahedrally coordinated nickel(II) complexes and can be classed into two types: (i) NiN_4ox: the four coordinated atoms different to the two O-(oxalate) atoms are N-amine atoms and the -J values in all cases are in the 32.4–39 cm^{-1} range [1, 3–6]. Four complexes of this kind have been structurally characterized [4–7]. (ii) NiN_3Oox: three of the four coordinated atoms different to the O-(oxalate) are N-amine atoms and the fourth is an O-(H_2O) atom. Only two compounds of this type [2, 8], (μ-ox)[Ni(dien)(H_2O)]$_2$(ClO_4)$_2$, where dien is diethylenetriamine and (μ-ox)[Ni(L)(H_2O)](NO_3)$_2$·2H_2O, where L is 1,4,7-triazacyclononane (structurally characterized), have been magnetically studied, showing J values of −24.4 and −25.5 cm^{-1}, respectively.

The lower coupling parameter J for these NiN_3Oox compounds is clearly anomalous compared with the wide series of NiN_4ox oxalato dimers, for which in the most recent papers, J values near −35 cm^{-1} are considered routine results taking into account two factors: first, the oxalato bridge is always planar and very rigid, and no significant differences in the bond angles or bond distances that may influence the superexchange should be expected; second, the coordination environment of nickel(II) ion in this kind of complex is always octahedral and consequently a weak influence of the electronic effects due to the orientation of the d orbitals of the nickel(II) can be expected.

The aim of this work is to synthesize compounds of the NiN_3Oox type and to perform structural, magnetic and MO studies to determine the influence on the magnetic coupling caused by the substitution of one N-coordinated atom by one O atom in the peripheral ligands. With this in mind, starting from triaza ligands,

*Author to whom correspondence should be addressed.

SSDI 0020-1693(93)03731-O

we synthesized the (μ-ox)[Ni(dpt)(H_2O)]$_2$(ClO_4)$_2$ (**1**), (μ-ox)[Ni(Medpt)(H_2O)]$_2$(ClO_4)$_2$ 2H_2O (**2**) and (μ-ox)[Ni(ept)(H_2O)]$_2$(ClO_4)$_2$ (**3**) compounds, where dpt is bis(3-aminopropyl)amine, Medpt is 3,3'-diamino-*N*-methyl-dipropylamine and ept is *N*-(2-aminoethyl)-1,3-propanediamine. The synthesis of **1** has been previously described in the literature [9] but without any magnetic or structural study The crystal structure of **1** and **2** was determined. Variable temperature magnetic susceptibility measurements were performed in the range 300–4 K: the resulting data show that these NiN_3Oox compounds are antiferromagnetically coupled, but the coupling is significantly lower than in the case of the dinuclear analogous NiN_4ox compounds and very close to the two NiN_3Oox systems previously reported. This series of five NiN_3Oox complexes suggests that these lower J values are characteristic of this nickel(II) environment and not anomalous results. Extended-Huckel MO calculations have been performed on the structurally characterized dinuclear complexes in an attempt to understand the variation in the magnetic coupling as a function of the resulting energy levels

Experimental

Caution: Perchlorate salts of metal complexes are potentially explosive Only a small amount of material should be prepared, and it should be handled with caution.

Preparation of the new complexes

(μ-ox)[Ni(dpt)(H_2O)]$_2$(ClO_4)$_2$ (**1**) was synthesized by the method reported by Curtis [9]. The new compounds (μ-ox)[Ni(Medpt)(H_2O)]$_2$(ClO_4)$_2$·2H_2O (**2**) and (μ-ox)[Ni(ept)(H_2O)]$_2$(ClO_4)$_2$ (**3**) were synthesized by the same method but using Medpt or ept instead of dpt. Monocrystals suitable for X-ray diffraction were obtained by slow air evaporation of diluted aqueous solutions of **1** and **2**. All attempts to obtain monocrystals of compound **3** were unsuccessful. Satisfactory analytical results (C, H, N, Cl), were obtained for all the complexes.

Techniques

IR spectra (4000–200 cm^{-1}) were recorded from KBr pellets in a Perkin–Elmer 1330 IR spectrophotometer. Magnetic measurements were carried out on polycrystalline samples with a pendulum type magnetometer (MANICS DSM8) equipped with a helium continuous-flow cryostat working in the temperature range 300–4 K, and a Brucker BE15 electromagnet. The magnetic field was close 15 000 G. For all compounds, the independence of the magnetic susceptibility versus the applied field was checked at room temperature until 1.8 T. Calibration of the instrument was made by a magnetization measurement of a standard ferrite. Diamagnetic corrections were estimated from Pascal constants

X-ray structure determination

Crystals (0.1×0.1×0.1 mm) of **1** and (0.2×0.2×0.2 mm) of **2** were selected and mounted on an Enraf-Nonius CAD4 four-circle diffractometer equipped with a graphite monochromator The unit-cell parameters were obtained by least-squares refinement of the setting angles of 25 reflections in the range $8<\theta<15°$. No significant change was detected in the intensity of the three standard reflections. Lorentz, polarization and absorption corrections were applied to the data (empirical method, psi-scan). The crystallographic data are shown in Table 1. The crystal structure was solved by Patterson synthesis using the SHELXS computer program. The two structures were refined by the full-matrix least-squares method, using the SHELX76 [10], CRYSTAL [11] AND PLATON [12] computer programs. The functions minimized were $R=\Sigma[|F_o|-k|F_c|]/\Sigma|F_o|$ and $R_w=[\Sigma w(|F_o|-k[F_c])^2/\Sigma w|F_o|^2]^{1/2}$. f, f', and f'' were taken from International Tables of X-Ray Crystallography [13]. Positions of H atoms were computed and refined with an overall isotropic factor, using a riding model. For **1** the final R factor was 0.063 ($R_w=0.068$). Number of parameters refined = 170 Max. shift/e.s d. = 0.15; max. peak in final difference synthesis was 0.5 e $Å^{-3}$. For **2**, the final R factor was 0 063 ($R_w=0$ 068)

TABLE 1 Crystallographic data for (μ-ox)[Ni(dpt)(H_2O)]$_2$(ClO_4)$_2$ (**1**) and (μ-ox)[Ni(Medpt)(H_2O)]$_2$(ClO_4)$_2$ 2H_2O (**2**)

	1	**2**
Formula	$C_{14}H_{38}Cl_2N_6Ni_2O_{14}$	$C_{16}H_{46}Cl_2N_6Ni_2O_{16}$
Formula weight	702 8	766 9
Temperature (K)	293	293
Space group	*I2/a*	$P2_1/n$
a (Å)	12 534(4)	6 404(2)
b (Å)	16 871(5)	13 333(4)
c (Å)	13.450(4)	18 687(4)
β (°)	95 28(7)	97 67(8)
V ($Å^3$)	2831(3)	1576(2)
Z	4	2
λ (Mo Kα) (Å)	0 71069	0 71069
D_{calc} (g cm^{-3})	1 648	1 598
μ (Mo Kα) cm^{-1})	15.94	14.39
Absorption correction	empirical	empirical
Scan method	$\theta/2\theta$	$\theta/2\theta$
Reflections measured range $1\leqslant\theta\leqslant28°$	4911	5140
Reflections observed $I\geqslant3\sigma(I)$	2775	2460
$\pm h$, $\pm k$, $\pm l$	±16, 22, 17	±8, 18, 26
R^a	0 063	0 063
$R_w{}^b$	0 068	0 068

$^aR=\Sigma||F_o|-k|F_c||/\Sigma|F_o|$ $^bR_w=[\Sigma w(|F_o|-k|F_c|)^2/\Sigma w|F_o|^2]^{1/2}$.

for all observed reflections. The number of parameters refined was 191. Max. shift/e.s.d. = 0.1; max. peak in final difference syntheses was 0.6 e $Å^{-3}$. Final atomic coordinates for **1** and **2** are given in Tables 2 and 3, respectively.

TABLE 2 Final atomic coordinates and equivalent isotropic thermal parameters ($Å^2$) and their e s d.s for (μ-ox)[Ni(dpt)(H_2O)]$_2$(ClO_4)$_2$ (**1**)

	x/a	*y/b*	*z/c*	U_{iso}
Ni	0.09922(4)	0.07498(3)	0 35241(4)	0 0375(3)
Cl(1)	0.2500	0.3368(1)	0 5000	0 077(2)
Cl(2)	0.2500	−0.2071(1)	0 5000	0 072(1)
O(1)	0.1166(2)	0.0568(2)	0.5098(2)	0.041(2)
O(2)	−0 0372(3)	0.0074(2)	0 3723(2)	0 045(2)
O(3)	0.2475(3)	0 1371(2)	0 3573(3)	0 047(2)
O(10)	0.2967(9)	0.2922(6)	0 4358(8)	0 167(4)
O(11)	0.185(1)	0.393(1)	0 463(1)	0 287(8)
O(20)	0.1567(5)	−0 1597(4)	0 4867(5)	0 099(2)
O(21)	0.2552(9)	−0 2540(7)	0 4132(8)	0 172(4)
N(1)	0 0250(4)	0 1806(3)	0 3850(4)	0 057(3)
N(2)	0.1930(4)	−0 0253(3)	0 3352(3)	0 051(2)
N(3)	0.0681(4)	0.0878(3)	0.1992(3)	0 055(3)
C(1)	0.0437(3)	0 0145(3)	0.5400(3)	0 038(2)
C(2)	−0.016(1)	0.2380(7)	0 3115(9)	0 114(4)
C(3)	0.007(1)	0.2269(6)	0 2138(7)	0.098(4)
C(4)	−0.0155(8)	0.1486(7)	0 1690(6)	0 094(3)
C(5)	0.1562(6)	−0 0816(4)	0 2565(5)	0 069(4)
C(6)	0 1401(9)	−0.0437(5)	0 1562(6)	0 084(7)
C(7)	0 0485(7)	0.0140(5)	0 1442(5)	0 077(4)

TABLE 3. Final atomic coordinates ($\times 10^4$) and equivalent isotropic thermal parameters ($Å^2$) and their e s d.s for (μ-ox)[Ni(Medpt)(H_2O)]$_2$(ClO_4)$_2$ 2H_2O (**2**)

	x/a	*y/b*	*z/c*	U_{iso}
Ni	0.2449(1)	0.33262(6)	0.00703(4)	0 0246(3)
O(1)	0.5491(7)	0.3747(3)	−0.0190(2)	0 028(1)
O(2)	0.2557(7)	0.4887(3)	0 0319(3)	0 031(1)
O(3)	−0.0470(7)	0.3077(4)	0 0426(3)	0 037(1)
O(10)	0.902(1)	0.3279(6)	0.1842(4)	0 076(3)
N(1)	0.389(1)	0.3083(4)	0.1121(3)	0 037(2)
N(2)	0.0945(9)	0.3812(4)	−0 0927(3)	0 033(2)
N(3)	0.2539(8)	0.1808(4)	−0.0276(3)	0.032(2)
C(1)	0.584(1)	0 4671(5)	−0 0144(3)	0 028(2)
C(2)	0.375(1)	0 2103(7)	0.1476(4)	0 044(2)
C(3)	0.421(2)	0.1248(7)	0 0994(5)	0 052(3)
C(4)	0.257(1)	0.1082(6)	0 0339(5)	0.044(2)
C(5)	−0 062(1)	0.3175(6)	−0 1373(4)	0.039(2)
C(6)	0.020(1)	0.2141(6)	−0.1477(4)	0.042(2)
C(7)	0 063(1)	0.1526(6)	−0 0786(4)	0 041(2)
C(8)	0 443(1)	0.1640(6)	−0.0634(5)	0 045(2)
Cl(1)	0.5789(4)	0.5520(2)	0.2489(1)	0 0512(7)
O(4)	0.587(2)	0.6517(6)	0.2240(5)	0.095(4)
O(5)	0.773(2)	0.5030(9)	0.2578(8)	0 136(5)
O(6)	0.420(2)	0.5014(8)	0.219(1)	0 148(7)
O(7)	0.553(3)	0.563(1)	0.3209(6)	0 152(7)

Results and discussion

IR spectra

The IR spectra of the dinuclear complexes are very similar: the bands attributable to the peripheral ligands and the two strong characteristic bands attributable to the ClO_4^- anion appear at normal frequencies. The most characteristic band attributable to the central bridging oxalato ligand, appears at 1640 cm^{-1} (vs, broad) in all cases.

Description of the structures

(μ-ox)[Ni(dpt)(H_2O)]$_2$(ClO_4)$_2$ (1)

The unit cell contains four dinuclear [NiNi] dications and two symmetrically independent sets of perchlorate anions Selected bond lengths and angles are listed in Table 4. See also 'Supplementary material'. A view of the dinuclear unit with atom-labelling scheme is presented in Fig. 1(a) which shows the OH_2 ligands placed in the NioxNi plane in *trans* configuration. The nickel atom occupies a distorted octahedral environment: the Ni(1)–N(1), Ni(1)–N(2), Ni(1)–O(2) and Ni(1)–N(3)

TABLE 4 Selected bond lengths (Å) and angles (°) for (μ-ox)[Ni(dpt)(H_2O)]$_2$(ClO_4)$_2$ (**1**)

Ni(1)–O(1)	2 131(3)
Ni(1)–O(2)	2.092(3)
Ni(1)–O(3)	2.130(3)
Ni(1)–N(1)	2.075(5)
Ni(1)–N(2)	2.085(4)
Ni(1)–N(3)	2.072(4)
O(1)–C(1)	1.255(5)
O(2)–C(1)	1.247(5)
N(1)–C(2)	1 446(9)
N(2)–C(5)	1 465(8)
N(3)–C(4)	1 50(1)
N(3)–C(7)	1.458(9)
C(1)–C(1)′	1 542(8)
O(2)–Ni(1)–O(1)	78.7(1)
O(3)–Ni(1)–O(1)	91 8(1)
O(3)–Ni(1)–O(2)	170 2(1)
N(1)–Ni(1)–O(1)	85.4(2)
N(1)–Ni(1)–O(2)	93.0(2)
N(1)–Ni(1)–O(3)	88 7(2)
N(2)–Ni(1)–O(1)	89 2(2)
N(2)–Ni(1)–O(2)	92 8(2)
N(2)–Ni(1)–O(3)	84 4(1)
N(2)–Ni(1)–N(1)	171 2(2)
N(3)–Ni(1)–O(1)	174 6(2)
N(3)–Ni(1)–O(2)	95.9(2)
N(3)–Ni(1)–O(3)	93.6(2)
N(3)–Ni(1)–N(1)	94.2(2)
N(3)–Ni(1)–N(2)	91.7(2)
C(1)–O(1)–Ni(1)	113.1(3)
C(1)–O(2)–Ni(1)	114.1(3)
O(2)–C(1)–O(1)	126 0(4)
C(1)–C(1)–O(1)	116.5(4)
C(1)–C(1)–O(2)	117 5(5)

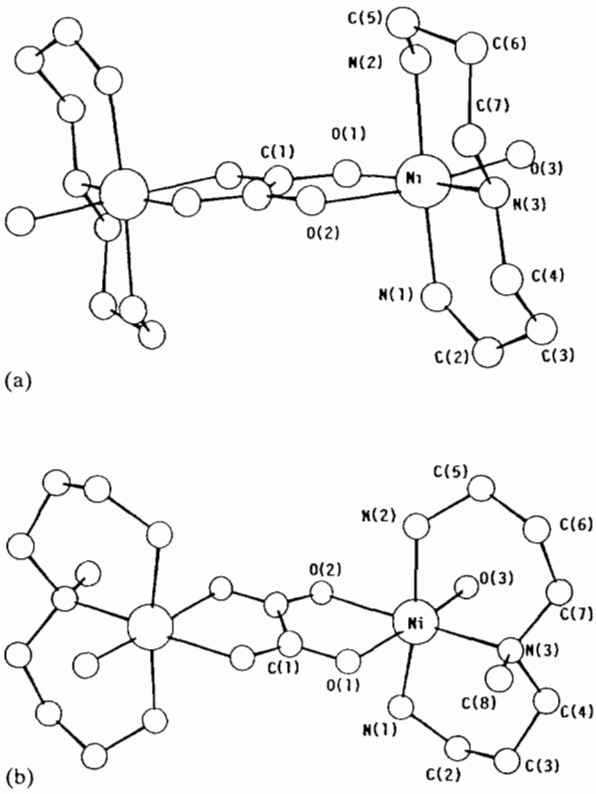

Fig. 1 Molecular structure of (a) $(\mu\text{-ox})[Ni(dpt)(H_2O)]_2^{2+}$, and (b) $(\mu\text{-ox})[Ni(Medpt)(H_2O)]_2^{2+}$, showing the atom labelling scheme.

distances are similar, and shorter than the other two Ni(1)–O(1) and Ni(1)–O(3). The nickel atom is placed 0.143 Å above the mean plane formed by the N(1), N(2), O(2) and O(3) atoms. N(3) is placed 2.215 Å above this mean plane and O(1) 1.973 Å on top. The nickel atom is placed 0.009 Å above the mean plane defined by Ni(1), O(1), O(2) and C(1), the nickel–oxalato–nickel fragment being planar. Dimeric entities are related by hydrogen bonds between O(1)–O(3)', distance 2.715 Å. The structure can be envisaged as an infinite zigzag chain as shown in Fig. 2(a). The perchlorate anions are also at hydrogen bond distances from O(3) (2.867 Å). The *trans* arrangement of the amine is different to that found in the related trinuclear compound $\{[Ni(dpt)(H_2O)]_2Cu(pba)\}^{2+}$ (pba = 1,3-propylenebis(oxamato)) in which the coordinated aquo ligands are placed in *cis* arrangement to the central Ni_2(pba)Cu plane [14].

$(\mu\text{-ox})[Ni(Medpt)(H_2O)]_2(ClO_4)_2 \cdot 2H_2O$ (2)

The unit cell contains two dinuclear [NiNi] dications and four perchlorate anions. Selected bond lengths and angles are listed in Table 5. See also 'Supplementary material'. A view of the dinuclear unit with atom-labelling scheme is presented in Fig. 1(b) which shows the OH_2 ligands placed in the NioxNi plane in *trans*

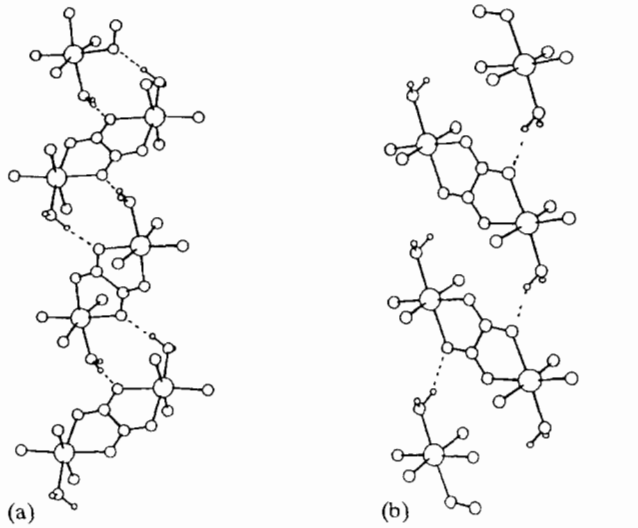

Fig 2 (a) Infinite zigzag chains of dimeric units of $(\mu\text{-ox})[Ni(dpt)(H_2O)]_2^{2+}$ (**1**) and (b) infinite double chain of $(\mu\text{-ox})[Ni(Medpt)(H_2O)]_2^{2+}$ (**2**), linked by hydrogen bonds which are indicated by dotted lines

TABLE 5. Selected bond lengths (Å) and angles (°) for $(\mu\text{-ox})[Ni(Medpt)(H_2O)]_2(ClO_4)_2\ 2H_2O$ (**2**)

Ni(1)–O(1)	2.147(4)
Ni(1)–O(2)	2 132(5)
Ni(1)–O(3)	2 095(5)
Ni(1)–N(1)	2 078(6)
Ni(1)–N(2)	2 080(5)
Ni(1)–N(3)	2 128(6)
O(1)–C(1)	1 254(8)
O(2)–C(1)	1 264(8)
N(1)–C(2)	1 47(1)
N(2)–C(5)	1 479(9)
N(3)–C(4)	1 50(1)
N(3)–C(7)	1 492(9)
C(1)–C(1)'	1 54(1)
O(2)–Ni(1)–O(1)	77 9(2)
O(3)–Ni(1)–O(1)	172 2(2)
O(3)–Ni(1)–O(2)	95 1(2)
N(1)–Ni(1)–O(1)	87.4(2)
N(1)–Ni(1)–O(2)	87.1(2)
N(1)–Ni(1)–O(3)	88 7(2)
N(2)–Ni(1)–O(1)	92 3(3)
N(2)–Ni(1)–O(2)	83 6(2)
N(2)–Ni(1)–O(3)	90 5(2)
N(2)–Ni(1)–N(1)	170 5(2)
N(3)–Ni(1)–O(1)	96.7(2)
N(3)–Ni(1)–O(2)	173 5(2)
N(3)–Ni(1)–O(3)	90 5(2)
N(3)–Ni(1)–N(1)	96 4(2)
N(3)–Ni(1)–N(2)	93 0(2)
C(1)–O(1)–Ni(1)	113 6(4)
C(1)–O(2)–Ni(1)	113 7(4)
O(2)–C(1)–O(1)	125.7(6)
C(1)–C(1)–O(1)	117.1(7)
C(1)–C(1)–O(2)	117.2(7)

configuration as was the case for **1**. The nickel atom occupies a distorted octahedral environment: the Ni(1)–N(1), Ni(1)–N(2) and Ni(1)–O(3) distances are similar, and shorter than the other three distances Ni(1)–O(1), Ni(1)–O(2) and Ni(1)–N(3). The nickel atom is placed 0.153 Å above the mean plane formed by the N(1), N(2), O(1) and O(3) atoms. N(3) is placed 2.277 Å above this mean plane and O(2) 1.953 Å on top. As occurs in compound **1** the nickel–oxalato–nickel system is practically planar. The nickel atom is placed 0.041 Å out of the plane determined by Ni(1), O(1), C(1) and O(2) and O(3). This plane is practically perpendicular to the N(1), N(2), O(1) and O(3) plane (86.5°). A hydrogen bond, distance 2.698 Å is found between O(3) and O(10). There is also a hydrogen bond that relates two dinuclear entities: distance O(3)–O(1), is 2.831 Å. The structure can be seen as an infinite octahedral double chain through O(1) and O(3) using the hydrogen bonding (Fig. 2(b)). The Ni–O(oxalate), C–C(oxalate) and Ni–N(amine) distances and the C(oxalate)–C(oxalate)–O(oxalate) angle are similar in both structures to the published values for NiN_4O_2 compounds [4–7]. Only the O(oxalate)–Ni–O(oxalate) angle, 78.7(1)° for **1** and 77.9(2)° for **2**, is slightly lower than the analogous published values.

Magnetic properties

The χ_M versus T plots for complexes **1–3** are shown in Fig. 3. The χ_M values first increase, reaching a maximum at 32 K for **1**, 29.4 K for **2** and 35 K for **3**, and then decrease. This behaviour is typical of an antiferromagnetically coupled Ni(II)Ni(II) pair. Applying the isotropic spin Hamiltonian $\mathscr{H} = -JS_AS_B$ where J is the exchange integral and $S_A = S_B = 1$, the expression [15] for χ_M is:

$$\chi_M = \frac{(2N\beta^2g^2/KT)^*(2\exp(x) + 10\exp(3x))}{1 + 3\exp(x) + 5\exp(3x)}$$

In this expression N, β, K and g have their usual meaning and $x = J/kT$.

The zero-field splitting, D, has not been considered since the effect of D on the magnetic behaviour of this kind of compound can be neglected due to the large stabilization of the singlet ground state, and therefore, the slight influence of D does not change the position of the maximum and this position determines the J value [1, 5, 16].

Least-squares fitting of the magnetic data leads to the parameters given in Table 6. The minimized function was $R = \Sigma(\chi_M^{calc} - \chi_M^{obs})^2/\Sigma(\chi_M^{obs})^2$, and in all cases R was less than 10^{-4}. The J values show that the overlap between the magnetic orbitals is efficient, but it is lower than in the cases where the terminal ligands are two bidentate or one tetradentate amine, as can be seen in Table 6.

Two factors can contribute to these low J values: first, the hydrogen bonds between oxygen atoms of the coordination sphere of the nickel atoms and second, the presence of a coordinated water molecule *trans* to the oxalato bridge. The first factor has been studied [17–20] in series of copper(II) compounds and moderate $-J$ values due exclusively to the hydrogen bond have been found for short O–H–O distances (*c.* 2.4 Å) and for greater distances the $|J|$ value decreases very quickly.

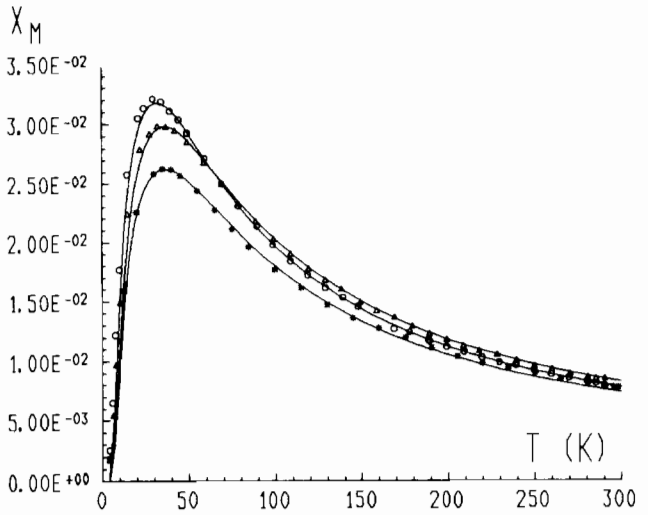

Fig. 3. Experimental and calculated (——) temperature dependence of χ_M for the dinuclear compounds (μ-ox)[Ni(dpt)$(H_2O)]_2(ClO_4)_2$ (**1**) (△), (μ-ox)[Ni(Medpt)$(H_2O)]_2(ClO_4)_2$ $2H_2O$ (**2**) (○) and (μ-ox)[Ni(ept)$(H_2O)]_2(ClO_4)_2$ (**3**) (*)

TABLE 6. Magnetic parameters (J in cm^{-1}) for dinuclear nickel(II)–oxalato systems

Compound[a]	J	g	Reference
NiN_4ox environment			
(μ-ox)[Ni(CTH)]$_2(ClO_4)_2$	−36.8	2.19	1
(μ-ox)[Ni(trien)]$_2(ClO_4)_2$	−35.2	2.20	1
(μ-ox)[Ni(en)$_2$]$_2(ClO_4)_2$	−36.8	2.27	3
(μ-ox)[Ni(tmd)$_2$]$_2(ClO_4)_2$	−36.4	2.18	4
(μ-ox)[Ni(nn')$_2$]$_2(ClO_4)_2$	−32.4	2.19	4
(μ-ox)[Ni(cyclam)]$_2(NO_3)_2$	−39.0	2.33	5
(μ-ox)[Ni(cyclen)]$_2(NO_3)_2$	−35.0	2 30	6
(μ-ox)[Ni(Me$_2$cyclen)]$_2(ClO_4)_2$	−34.0	2 15	6
NiN_3Oox environment			
(μ-ox)[Ni(dien)$(H_2O)]_2(ClO_4)_2$	−24.4	2.07	2
(μ-ox)[Ni(L)$(H_2O)]_2(NO_3)_2$	−25 5	2.10	8
(μ-ox)[Ni(dpt)$(H_2O)]_2(ClO_4)_2$	−24.7	2.32	this work
(μ-ox)[Ni(Medpt)$(H_2O)]_2(ClO_4)_2$	−21.6	2 24	this work
(μ-ox)[Ni(ept)$(H_2O)]_2(ClO_4)_2$	−25.0	2.19	this work

[a]Reference ligands are: (CTH) 2,4,4,9,9,11-hexamethyl-1,5,8,12-tetraazacyclotetradecane, (trien) triethylenetetramine, (en) 1,2-diaminoethane, (tmd) 1,3-diaminopropane, (nn') *N,N'*-quinolinethylenediamine, (cyclam) 1,4,8,11-tetraazacyclotetradecane, (cyclen) 1,4,7,10-tetraazacyclododecane, (Me$_2$cyclen) 1,7-dimethylcyclen, (dien) diethylenetriamine, (L) 1,4,7-triazacyclononane.

In our case, the O–H–O distances lie in the 2.7–2.8 Å range and the magnetic orbitals of the nickel entities are not coplanar and, consequently, the influence in the magnetic behaviour should be negligible. The very good fit at low temperatures of the plot of susceptibility versus temperature (Fig. 3), confirms that the intradimer superexchange should be due only to the intradimer interaction. The second factor needs a wider interpretation and extended-Huckel MO calculations to correlate the magnetic behaviour are described below.

MO calculations

The influence of size and electronegativity of the bridging ligand atoms on the intensity of the magnetic coupling has been well established by Verdaguer *et al.* [21, 22] for dinuclear systems of copper(II) for the series of bridging oxalate, oxamate and oxamidate ligands. In this study, good correlation was found between the coupling J parameter and the mixing coefficients of each orbital of the bridging atoms bound to the copper, maintaining the coefficients of the peripheral ligands as a constant. The conclusion is that less electronegative bridging atoms permit larger delocalization of spin density on the bridge, better overlap between magnetic orbitals and larger antiferromagnetic coupling.

Taking into account that the contribution to the total energy of the resulting molecular orbitals is similar for bridging and peripheral ligands, a possible explanation for the lower J values in the NiN_3Oox systems compared with the NiN_4ox analogous systems can be given in the same way, but in our case the constant parameters are those related with the oxygens of the oxalato group, and the variable parameters are those related with the ligands placed *trans* to the bridging bonds (xy plane).

To check this explanation, extended-Hückel MO calculations were performed on the structurally characterized dinuclear complexes using the CACAO program [23]. The atomic parameters used for nickel, C, O, N and H were the standards of the program.

In order to centre this analysis on the coordination environment of the nickel(II) cations, according to the two structural examples available, the geometry was modelized placing the nickel atoms in a slightly distorted octahedral environment, as shown below:

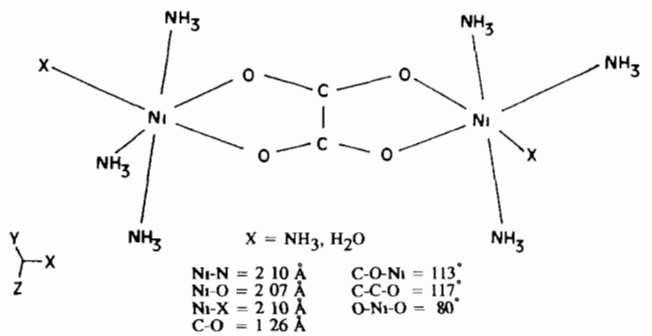

For a dimeric nickel(II) system with two unpaired electrons on each metal atom, four molecular orbitals ϕ_1, ϕ_2, ϕ_3 and ϕ_4 (ϕ_1 and ϕ_2 with z^2 and ϕ_3 and ϕ_4 with xy as main contribution), are expected. The MO diagram for the four significant orbitals is shown in Fig. 4. For this system with spin states $S=0$, 1, 2, $E_2-E_1=-2J$ and $E_1-E_0=-J$, in which $2J=K-V$, where K is a ferromagnetic term of bielectronic integrals and V an antiferromagnetic term, which can be described [24] as a function of the splitting of the pairs of molecular orbitals as follows:

$$V=1/2(\epsilon_1-\epsilon_2)^2/(J_{aa}-J_{ac})+1/2(\epsilon_3-\epsilon_4)^2/(J_{bb}-J_{bd})$$

J_{mn} being bielectronic integrals, all assumed to be constant in a series of complexes of similar geometry.

The calculated square gaps ($\Delta^2=\Sigma(\epsilon_i-\epsilon_j)^2$, eV^2), for the z^2 and xy pairs of molecular orbitals are 3.7×10^{-3} and 1.4×10^{-2} for the NiN_4ox environment and 1.9×10^{-3} and 7.2×10^{-3} in the NiN_3Oox environment. The smaller z^2 splitting compared with the xy splitting can be attributed to the more favourable xy ligand overlap and, as expected, the main contribution to the antiferromagnetic coupling is due to the gap between the xy pair of molecular orbitals. By using this semiempirical model, the absolute values of these splittings are not significant and their importance lies in their gradation when some parameters are changing. If we assume all

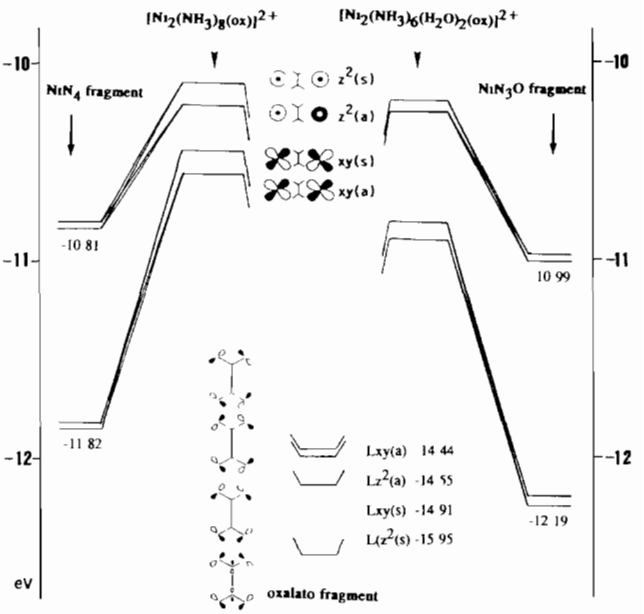

Fig. 4. Interaction diagram for selected metal and oxalato fragment lone pair orbitals for (μ-ox)[Ni(NH$_3$)$_4$]$_2^{2+}$ system (left) and (μ-ox)[Ni(NH$_3$)$_3$(H$_2$O)]$_2^{2+}$ system (right). The four resulting MOs are schematized indicating the main oxalato contribution. Energy of the corresponding levels are −10.10, −10.16, −10.44 and −10.56 eV for the (μ-ox)[Ni(NH$_3$)$_4$]$_2^{2+}$ system and −10.17, −10.22, −10.81 and −10.90 eV for the (μ-ox)[Ni(NH$_3$)$_3$(H$_2$O)]$_2^{2+}$ system

the other factors as constant, $\Sigma\Delta^2$ is 9.2×10^{-3} for NiN_3Oox, and 1.7×10^{-2} for NiN_4ox. These results indicate larger antiferromagnetic values of the coupling $|J|$ parameter as a function of the electronegativity of peripheral ligands, in the order O < N, that is to say, it is the same result as that reported by Verdaguer *et al.* [21] when the electronegativity changes are located in the bridging ligand. This approach corresponds to the experimental decrease of $|J|$ when an N-amine atom is substituted by an O-atom of a water molecule, and shows a new example of tuning the magnetic properties of dinuclear nickel complexes. In this way, maintaining the oxalate bridging ligand, the calculations for a limit case in which the four peripheral ligands are less electronegative, such as sulfur atoms (taking a distance Ni–S of 2.25 Å), gives a $\Sigma\Delta^2$ value of 0.097. This value must indicate a very high antiferromagnetic coupling for an S_4Ni–ox–NiS_4 system, and current efforts are being made in our laboratory to synthesize Ni(II) dinuclear μ-oxalate compounds with terminal S-ligands to corroborate this approach.

Supplementary material

Further data (atomic fractional coordinates, complete distances and angles, etc.) can be obtained on request from the Crystallographic Data Centre, University Chemical Laboratory, Lensfield Road, Cambridge CB2 1EW, UK.

Acknowledgement

We are very grateful for the financial assistance from the CICYT (Grant No. PB88/0197).

References

1 D M. Duggan, E.K. Barefield and D.N. Hendrickson, *Inorg Chem*, *12* (1973) 985
2 T R Felthouse, E J Laskowski and D N Hendrickson, *Inorg Chem*, *16* (1977) 1077.
3 V V. Zelentsov, L.M. Chanturiya and N.I. Pirtskhalava, *Koord Khim*, *4* (1978) 764
4 J. Ribas, M. Monfort, C Diaz and X. Solans, *An Quím*, *84* (1988) 186.
5 L.P Battaglia, A. Bianchi, A Bonamartini Corradi, E Garcia-España, M Micheloni and M. Julve, *Inorg Chem.*, *27* (1988) 4174
6 A. Bencini, A. Bianchi, E Garcia-España, Y. Jeannin, M Julve, V. Marcelino and M Philoche-Levisalles, *Inorg Chem*, *29* (1990) 963.
7 N.F Curtis, I.R.N McCormick and T N. Waters, *J Chem. Soc, Dalton Trans.*, (1973) 1537.
8 A. Bencini, A. Bianchi, P Paoli, E Garcia-España, M. Julve and V. Marcelino, *J. Chem Soc, Dalton Trans*, (1990) 2213
9 N.F. Curtis, *J Chem. Soc A*, (1968) 1584.
10 G M Sheldrick, *A Computer Program for Crystal Structure Determination*, University of Cambridge, UK, 1976.
11 D J. Watkin, J.R Carruthers and P W. Betteridge, *Crystals Users Guide*, Chemical Crystallography Laboratory, University of Oxford, UK, 1985.
12 A.L. Spek, *Platon-90*, Vakgroep Algemene Chemie, University of Utrecht, Afdeling Kristal en Structuurchemie, Utrecht, Netherlands, 1990
13 *International Tables for X-ray Crystallography*, Kynoch, Birmingham, UK, 1974.
14 J Ribas, C. Diaz, R Costa, Y. Journaux, C. Mathoniere, O Kahn and A Gleizes, *Inorg Chem.*, *29* (1990) 2042
15 C J O'Connor, *Prog Inorg Chem*, *29* (1982) 203
16 A.P Ginsberg, R.L. Martin, R W. Brookes and R C. Sherwood, *Inorg Chem*, *11* (1972) 2884
17 J.A. Bertrand, E Fujita and D.G. VanDerveer, *Inorg Chem*, *19* (1980) 2022.
18 F. Nepveu, S Gehring and L Walt, *Chem Phys Lett*, *128* (1986) 300.
19 H. Muhonen, *Inorg Chem*, *25* (1986) 4692.
20 U Auerbach, T. Weyhermuller, K Wieghardt, B Nuber, E. Bill, C. Butzlaff and A X Trautwein, *Inorg Chem*, *32* (1993) 508.
21 M. Verdaguer, O. Kahn, M. Julve and A Gleizes, *Nouv. J Chim*, *9* (1985) 325.
22 R Vicente, J. Ribas, S Alvarez, A. Seguí, X Solans and M Verdaguer, *Inorg. Chem*, *26* (1987) 4004.
23 C Meallı and D.M. Proserpio, *J Chem Educ*, *67* (1990) 3399.
24 P.J. Hay, J C Thibeault and R. Hoffmann, *J Am Chem Soc*, *97* (1975) 4884.